Development of a powered grasping device for home-based neurorehabilitation

T. Feiler, Biomechatronic Systems, Fraunhofer IPA, Stuttgart, Germany, thomas.feiler@ipa.fraunhofer.de
F. Starker, Biomechatronic Systems, Fraunhofer IPA, Stuttgart, Germany
F. Dennerlein, Biomechatronic Systems, Fraunhofer IPA, Stuttgart, Germany
Dr. med. U. Schneider, Biomechatronic Systems, Fraunhofer IPA, Stuttgart, Germany
Dr.-Ing. B. Budaker, Biomechatronic Systems, Fraunhofer IPA, Stuttgart, Germany
Dr. med. S. R. Soekadar, Psychiatry and Psychotherapy, University Hospital, Tübingen, Germany
M. Witkowski, Psychiatry and Psychotherapy, University Hospital, Tübingen, Germany

Abstract

Introduction

The project “EU-Way” funded by the EC aims to develop and clinically evaluate non-invasive technologies that create bidirectional physiological links between a hand assistive device (like a prosthesis or an exoskeleton) and the patient's volition. These links will be achieved by means of interfaces based on novel principles that combine multilevel biosignals and multimodal sensory feedback.
For clinical evaluation, a simple powered orthotic training device for patients with paralysed upper limb (e.g. after stroke) was developed. The powered hand-orthosis in combination with biosignal control strategy and biofeedback represents a novel rehabilitation solution assisting patients during daily trial to prevent further spasticism and contractions.

Methods

The orthotic system consists out of an individual lightweight bracing based on 3d scanning technology covering wrist and forearm. On the dorsal side of the forearm an electromechanical drive system including a control unit is integrated in the bracing. Proper finger motion is realised by one actuator allowing for flexion and extension with help of elastic Bowden cables that are linked to a rocker mechanism. The rotatory motion of the motor is transformed to a linear movement using a ball screw mechanism. Moreover, a teach-in process facilitates for individual adaptation with regard to different disability levels of the patients. A universal and efficient bracing mount is designed to deal with various types of patients. Interaction between human and orthosis is realised by using a brain-computer-interface that is controlled directly by human biosignals (EEG, EMG).

Results

The system allows for variation of training modes with grasping forces up to 30 N as well as individualized motion patterns. Maximum range of motion realised by the setup is 0° extension and 90° flexion as a combined motion metacarpophalangeal joint and proximal interphalagenal joint. Test results with a functional prototype will be presented and discussed.

A comparative in vitro study of different non-thermal atmospheric pressure plasma-jets regarding their antimicrobial potential and destruction of bacterial biofilms

K. Wegner [1], K. Duske[2], J. B. Nebe[2], R. Bussiahn[4], A. Podbielski[3], R. Bader[1]

[1] Department of Orthopaedics, University Medical Center Rostock, Doberaner Str. 142, 18057 Rostock, Germany
[2] Department of Cell Biology, University Medical Center Rostock, Schillingallee 69, 18057 Rostock, Germany
[3] Institute of Medical Microbiology, Virology and Hygiene, University Medical Center Rostock, Schillingallee 70, 18057 Rostock, Germany
[4] Leibniz-Institute for Plasma Science and Technology (INP) Greifswald, Felix-Hausdorff-Str. 2, 17489 Greifswald, Germany

katharina.wegner@med.uni-rostock.de; kathrin.duske@med.uni-rostock; barbara.nebe@med.uni-rostock;bussiahn@inp-greifswald.de; andreas.podbielski@med.uni-rostock; rainer.bader@med.uni-rostock.de

Introduction

Implant-related infections can occur after total joint replacement [1]. Non-thermal atmospheric pressure plasma-jets with an admixture of chemically active gases might be an extension in the therapy of implant-related infections caused by bacterial biofilms to dispense an exchange of the implants. The objective of this experimental study was the comparison of five different non-thermal atmospheric pressure plasma-jet sources for their time-dependent antimicrobial potential and efficacy in the removal of bacterial biofilms.

Methods

For the experiments, biofilms of *S. epidermidis* ATCC 35984 were grown on sterile Polystyrene-cover slips (Ø 13 mm) in Caso-Bullion (37 °C, 5 % CO_2) prior to plasma-treatment, using five non-thermal atmospheric pressure plasma jets (kHz-Jet, kINPen08, kINPen09, kINPen Med [2]) and a dielectric barrier discharge (DBD). The biofilms were subjected to varying durations (1, 3 and 5 min) of argon plasma exposure, supplemented with 1 % O_2. Only the DBD operated with atmospheric air. Planctonic and biofilm-bound bacteria were quantified by assignment of viable bacterial counts. In addition, bacterial biofilms were observed by fluorescence microscopy and scanning electron microscopy (SEM) after plasma-treatment.

Results

After 5 min of plasma exposure, a reduction of vital planctonic and biofilm-bound bacteria (99 % and 90 % respectively), was observed for all plasma sources besides the DBD. Furthermore, it has been shown, that only the plasma sources kHz-Jet and kINPen08 show particularly striking results in the reduction of vital planctonic and biofilm-bound bacteria by up to two orders of magnitude already after 1 min of plasma exposure. Live/dead fluorescence examinations and SEM analysis confirmed this observation.

Conclusion

Our in vitro results demonstrate the possibility of biofilm removal and reduction of vital bacteria within the biofilm using non-thermal atmospheric pressure plasma-jets with specific characteristics Biofilm removal and reduction of vital bacteria using the kHz-Jet and the kINPen08 on different implant surfaces and materials will be subject to further investigations.

References

[1] W. Zimmerli, A. Trampuz, and P.E. Ochsner, *N Engl J Med*. 351(16): 1645-54, 2004.
[2] R. Bussiahn, N. Lembke, R. Gesche, T. von Woedtke, and K.D. Weltmann, *Hyg Med*. 38 (5): 212-216, 2013.

Development of a Smart Walker with a Vibrating Belt for Assisting Visually Impaired

M. Reyes Adame[1], A. Wachaja[2], P. Agarwal[2], W. Burgard[2], K. Moeller[1],
[1] Institute of Technical Medicine, Furtwangen University, Villingen-Schwenningen, Germany, rey@hs-furtwangen.de
[2] Institute of Computer Science, University of Freiburg, Freiburg, Germany

Introduction

A high number of elderly people suffer from walking disabilities in combination with visual impairment. Therefore current research in the field of Ambient Assisted Living focuses on extending the user's environmental perception using external sensors. Unlike existing approaches which are mainly limited to indoor use, we present a smart walker that can be used for both indoor and outdoor scenarios. It is an end-to-end system which detects potential obstacles and transmits the environmental information to a user through a vibrating belt.

Methods

Our system consists of a walker equipped with two planar laser range finders and a waist belt with an array of wirelessly controlled vibration motors. One range finder is used for localizing the walker employing scan matching methods. The second one is tilted up and down continuously by an attached servomotor to create a three-dimensional representation of the environment. This enables us to detect obstacles in the user's vicinity. To avoid potential collisions, distances to the detected obstacles in different angular regions are transmitted by vibrating different motors on the belt.

Results

The presented system is currently able to detect obstacles like people, walls and furniture. First hardware-in-the-loop experiments with the vibration belt in a simulated indoor environment showed that young non-disabled blindfolded test subjects could avoid collisions by receiving vibrating signals indicating the obstacle location.

Conclusion

We presented an end-to-end obstacle avoidance system for visually impaired elderly people based on 3D sensing technology and vibrating signals on the body. Current efforts are directed towards a complete system integration and the planning of extended experiments with visually and mobility impaired people.

Acknowledgment

This work has partially been supported by the Federal Ministry of Education and Research (BMBF) under grant no. 13EZ1129A (*i*VIEW), the European Regional Development Fund (ERDF) and the German State Ministries for Research of Baden-Württemberg (MWK) for the project ZAFH-AAL.

Forearm motor point characterization for smart electrode array shaping

A. Reinert, J. Loitz, W. Krautschneider, D. Schröder, Institute of Nanoelectronics, Hamburg University of Technology, Hamburg, Germany, a.reinert@tuhh.de, jan.loitz@tuhh.de

Introduction

For stroke patients that lack control of their hand, neuromuscular electrical stimulation has been proposed for treatment. Appropriate placement of the electrodes is a key factor for successful and efficient ways of electrical stimulation. Therefore a method for reliable and fast placement is desired. There are two approaches to improve electrode placement. The first is an electrode sleeve [1], the second an electrode array [2]. For optimal stimulation the position of the motor point for each muscle has to be identified.

Methods

In this paper the motor points of the forearm of 30 individuals for four different movements were characterized with a method modified from [3]. Determining the exact position of the motor points has been achieved through systematic variation of the pen-electrode position, performed with biphasic rectangular pulses, currents between 8 and 20 mA and a frequency of 35 Hz.

Results

Results show a clustering of the motor points with low spread. It was found that the deviation of motor points in longitudinal and transversal direction is different, resulting in an elliptic stimulation area.

Conclusion

These findings lead to a well-defined area for each specific motor point that can be used to define optimized shapes of electrodes and electrode arrays.

[1] Rüdiger Rupp, Member, IEEE, Alex Kreilinger, Martin Rohm, Vera Kaiser and Gernot R. Müller-Putz
"Development of a non-invasive, multifunctional grasp neuroprosthesis and its evaluation in an individual with a high spinal cord injury"
34th Annual International Conference of the IEEE EMBS San Diego, California USA, 28 August - 1 September, 2012

[2] Nebojša M Malešević, Lana Z Popović Maneski, Vojin Ilić, Nikola Jorgovanović, Goran Bijelić, Thierry Keller and Dejan B Popović
"A multi-pad electrode based functional electrical stimulation system for restoration of grasp"
Journal of NeuroEngineering and Rehabilitation 2012, 9:66

[2] Marc Lawrence, Samuel Monteleone, Dr. Thierry Keller, Prof., Silvestro Micera
"Optimized electrode placement and improved EMG detection for a new textile grasping neuroprosthesis"
International Functional Electrical Stimulation Society Conference, Freiboug, Germany, vol. 13, pp. 409-411

Bubble point determination and calculation of the maximum pore size for hydrophilic membranes

J.-B. Matthies[1], A. Buchholz[1], W. Schmidt[2], F. Luderer[1], K.-P. Schmitz[1,2], N. Grabow[1]
[1]Institut for Biomedical Engineering, University of Rostock, Germany, Joern-Bo.Matthies@uni-rostock.de
[2] Institut for ImplantatTechnology and Biomaterials, Rostock-Warnemuende, Germany

Abstract

In this work, a novel test setup for bubble point determination of membranes is presented and tested. Different filtration systems were examined and compared with the manufacturer's information. Furthermore, a self-produced electrospun polyamide (PA 6) membrane was examined regarding its bubble point. Contact angle was measured and maximum pore size of the PA 6 membrane was calculated. Suitability of the setup for determining bubble point and the basis of calculation of maximum membrane pore size could be demonstrated.

1 Introduction

Infusion filters significantly reduce the rate of sepsis for high risk patients, for example in intensive paediatric therapy. [1] These filters separate small particles, such as glass, cotton particles and bacteria, from the administered medication. If the filter membrane is positively charged, retention of endotoxins is also achieved. [2] Depending on the application, infusion filters can be produced typically with either 0.2 micron pore size for the sterile filtration or 1.2 micron pore size for the administration of lipid containing suspensions. [2] Such filtration membranes have to pass several integrity tests regarding their functionality. In this work, the bubble point of selected membranes is tested with a self-developed test setup. The bubble point indicates the pressure, above which a wetted hydrophilic membrane is permeable to gas. It is of high importance in clinical application, because the infusion is administered under pressure and it must be ensured that no air bubbles enter the circulation. To test the functionality of the test setup, different infusion filter membranes were investigated. Based on this method, the maximum pore size of a membrane prepared by electrospinning of polyamide (PA 6) was determined. For this purpose, the contact angle of the membrane was measured with ultra pure water, and the pore size was determined as a function of the bubble point and surface tension.

2 Methods

2.1 Bubble Point Test Setup

Figure 1 shows the developed test setup with its components. The development and testing was conducted in accordance to the DIN 58355-2 standard. [3] The setup was designed to test complete filtration systems (filter housing, leads and filter membrane), as well as individual filter membranes. The application of pressure is achieved by a pressure regulator (SMC, Switzerland) with an accuracy of 0.5%. To determine the bubble point, the wetted filter is connected by a pressure-tight conduit and Luer-Lock connection to the pressure regulator. The pressure is increased in steps of 0.05 bar. The test parameters are listed in Table 1.

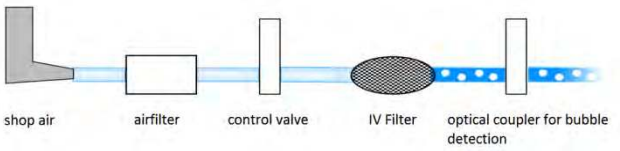

Figure 1 Schematic of the bubble point test setup

Table 1 Test parameters for bubble point testing

starting pressure	0.1 bar
pressure steps	0.05 bar
holding time	15 s

According to the standard, the bubble point is reached when a continuous bubble chain is detected at the filter outflow. This detection is realized by an optical coupler. A software calculates the average pressure of the last stage. The analysed filtration systems (RoweMed, Germany) are connected directly to the pressure regulator. The electrospun PA 6 membrane was placed in a suitable filter housing (polycarbonate syringe filter, Sartorius, Germany). The studied specimens and the main characteristics are listed in Table 2. At least six specimens were tested in each group.

Table 2 Tested filter membranes and main characteristics

filter type	membrane material	pore diameter as specified by the manufacturer [µm]	charge
RowePead	PET	1.2	n/a
RoweEpiflow	PET	0.2	n/a
RoweEpiflow	PA 6.6	0.2	+
electrospun membrane	PA 6	n/a	n/a

2.2 Contact Angle

To calculate the largest pore size of the PA 6 membrane, the contact angle against ultrapure water was measured with the sessile drop method with an OCA 20 (DataPhysics Instruments, Germany). The largest pore size was calculated considering the surface tension and wetting angle (Formula 1). A surface tension of water of 72.75 mN/m was used for the calculation. [4]

Formula 1 Calculation of the maximum pore size

$$D = \frac{4\sigma * \cos\theta}{\Delta p}$$

D : maximum pore size in µm
Δp : pressure difference (bubble point) in bar
σ : surface tension of the fluid in N/m
Θ : wetting angle of the fluid in °

3 Results

Measured bubble point data in comparison to manufacturer's data are given in Figure 2.

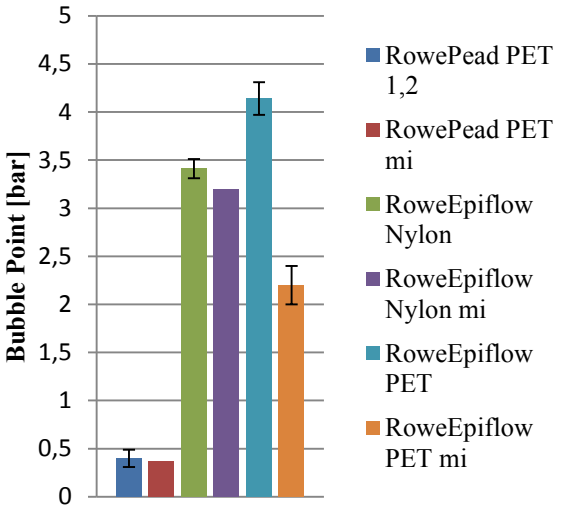

Figure 2 Bubble point data of the tested filtration systems in comparison to the manufacturer's information (mi)

In case of the filtration system RoweEpiflow with a 0.2 micron PET membrane, the value of the specified bubble point was determined by the manufacturer using ethanol. The bubble point of the electrospun PA 6 membrane was determined as 5.48 ± 0.11 bar. The measured contact angle of the PA 6 membrane was 30.2 ± 4.52°, which compares to 62.6° as literature data for a PA 6 film. [4] Calculated maximum pore size of the PA 6 membrane was 0.24/0.45 µm, based on the calculated/literature data of PA 6 contact angle, respectively.

4 Conclusion

The functionality of the developed test setup for determining the bubble point of membranes has been verified. Commercial filtration systems were investigated, and the measured data were compared with the manufacturer's data. No substantial differences were observed between the measured data and the data given by the manufacturer. Only the data for the filtration system RoweEpiflow with a 0.2 micron PET membrane could not be compared, because the manufacturer data was measured using 100 % ethanol. The developed test setup uses ultrapure water for the measurement. The expected differences between membranes with 0.2 and 1.2 micron pore size are clearly visible. The filtration systems with 1.2 micron pore size show a substantially lower pressure than filtration systems with 0.2 micron pore size. Since the bubble point of the filtration systems with 0.2 micron pore size are well above 1.2 bar, the systems are considered as safe for clinical use. Most clinical syringe pumps for infusion therapy shut off at a maximum pressure of 1.2 bar. [5] The self-produced PA 6 membrane was examined in the test setup with a polycarbonate syringe filter housing. In order to calculate the maximum pore size, the contact angle was measured with ultrapure water using the sessile drop method. It should be noticed that the measured value for the PA 6 membrane distinguishes approximately by a factor of two from the data reported in literature for a smooth PA 6 film (62.6/30.2° literature/measured). This can be attributed to the morphological features of a porous structure. As the water drop was absorbed by the pores of the membrane, no constant equilibrium was achieved. This also explains the smaller measured contact angle in comparison to the film. In general, the use of smooth films for the determination of contact angle is recommended for the calculation of maximum pore size. In conclusion, the functionality of the developed test setup for determining the bubble point was shown. The test setup can also be used as a basis for the calculation of maximum pore size.

5 Acknowledgements

This project was funded by the European Regional Development Fund (ERDF) and the European Social Fund (ESF) within the collaborative research between economy and science of the state Mecklenburg-Vorpommern.

5 References

[1] T. Jack, M. Boehme, B. E. Brent, et al: In-line filtration reduces severe complications and length of stay on pediatric intensive care unit: a prospective, randomized, controlled trial. Intensive Care Med 38:1008–16, 2012

[2] K. Bethune, M. Allwood, C. Grainger, C. Wormleighton: Use of filters during the preparation and administration of parenteral nutrition: position paper and guidelines prepared by a British pharmaceutical nutrition group working party. Nutrition 17:403–8, 2001

[3] DIN 58355-2, Membranfilter – Teil2: Prüfung des Blasendrucks, 2005

[4] http://www.chemie.de/lexikon/Oberfl%C3%A4chenspannung.html

[5] B. Braun Space Datasheet, 2005

Adaptive Control of Biomechanically Inspired Orthotic Exoskeleton in Paraplegic Rehabilitation

Preethika Immaculate Britto [a], Rekha Viajakumar Ph.D, Sudesh Sivarasu Ph.D [b*]

[a] School of Bio Sciences and Technology, VIT University, Vellore, India 632014
[b] MRC/MIRU – Division of Biomedical Engineering, Department of Human Biology, Faculty of Health Sciences, University of Cape Town, South Africa 7925. * - Sudesh.Sivarasu@uct.ac.za

Abstract:

The paper discusses the adaptive control mechanism used in a biomechanically inspired robotic exoskeleton which is designed to provide mobility assistance for paraplegic patients. This indigenous robot is manufactured at a low cost and highly suitable for developing nations such as India. One of the major problem with Robotic exoskeleton is the problem for controlling the weight transfer and balance in the exoskeleton during the full gait cycle. The paper describes an adaptive control algorithm, which will help to solve this key control issue.

1 Background

Lower extremity paralysis results in significant global morbidity and mortality. In India it is discovered that 3.96 percent of the population is "handicapped. Roughly 1% of the world's population relies on wheelchairs for mobility. With the aging of the population this number is skyrocketing. There are currently about 262,000 spinal cord injured (SCI) individuals in the United States, with roughly 12,000 new injuries sustained each year at an average age of injury of 40.2 years *[(2011). Spinal Cord Injury Facts and Figures at a Glance. https://www.nscisc.uab.edu]*. Of these, at least 44% (at least 5300 cases per year) result in paraplegia. One of the most significant impairments resulting from paraplegia is the loss of mobility, particularly given the relatively young (average) age at which such injuries occur. Surveys of persons with paraplegia indicate that mobility concerns are among the most prevalent [*R. W. Hanson and M. R. Franklin*], and that chief among mobility desires is the ability to walk and stand *[D. L. Brown-Triolo, M. J. Roach et.al]*. In addition to impaired mobility, the inability to stand and walk entails severe physiological effects, including muscular atrophy, loss of bone mineral content, frequent skin breakdown problems, increased incidence of urinary tract infection, muscle spasticity, impaired lymphatic and vascular circulation, impaired digestive operation, and reduced respiratory and cardiovascular capacities *[L. Phillips, M. Ozer et. al]*.

In an effort to restore some degree of legged mobility to individuals with paraplegia, several lower limb orthoses have been developed Although wheelchairs play a high role in paraplegic rehabilitation, the options for people with mobility disorders have been limited. Humans were not designed to sit for hours on end. *.(P. B. Butler, R. E. Major, et al)* The result of constant sitting is pressure sores, atrophied leg muscles and brittle bones. Wheelchair users are at elevated risk for carpal tunnel syndrome or repetitive strain injury from the constant impact of the hands against the push rims of the wheels. While wheelchairs offer people with mobility disorders freedom, it is not without its costs. *(R. Bogue et al)*

To solve the above mentioned issues robotics comes into the scenario. Exoskeletal robotics plays a promising role in rehabilitating paralyzed patients. As a part of rehabilitation robotics this paper aims at the development of a lower extremity biped exoskeleton to aid paralytic people. In order to be stable and robust, the exoskeleton must be a highly adaptable model, which is accomplished by integrating a perfect biomechanical design with computationally intelligent control. The exoskeletal prototype by itself stabilizes the posture, adaption to any terrain using robust gait paradigms.

2. Methods

The problem of realizing a full-fledged exoskeleton is accomplished by a biomechanically inspired mechanical design with a computationally intelligent control. The design comprises of a rigid exoskeletal structure which is actuated by a [1] Servo Controlled actuation unit, [2] Sensors for feedback and [3] a Micro Computing unit for achieving adaptive control. The sensor values from IMU (Inertial Measurement Unit) are obtained to infer the current position of robotic exoskeleton in 3-Dimensional space and are mapped with the control model involving the kinematics of the exoskeleton to obtain the control signals. The control inputs are converted into actuator output by a motor driving circuit that controls all 12 DOF actuators. This overall kinematic mechanism is monitored by torque angle sensors and position encoders that sends feedback to the controller to form a closed loop control. In order to make adaptive control robust and reliable the controller is chosen to meet a real-time standard that runs an optimized control program [Python based]. The mathematical control paradigm that runs behind all the hardware entities are evolved from the principles of Robot dynamics involving the solutions of the inverse kinematics as the control output, an adaptive model is evolved from ZMP (Zero moment point) calculation and Artificial neural networks for Gait generation and posture stability.

θ_1	$tan^{-1}\left(\frac{(d * sin\theta \cdot sin\alpha - sin\theta \cdot sin\alpha)}{(d * sin\theta \cdot sin\alpha - sin\theta \cdot sin\alpha) + l}\right)$

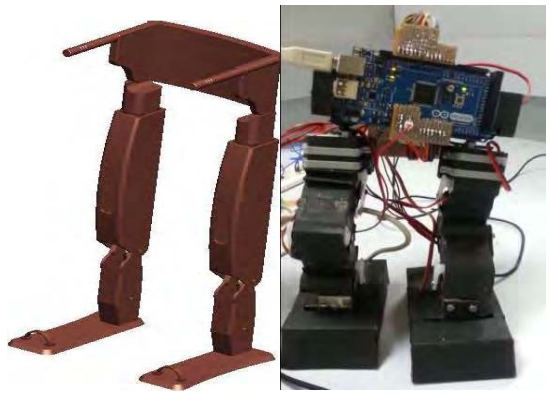

Fig 1-ProE design of the proposed exoskeleton, the tested Biped model prototype.

3. Results

Any kinematically constrained structure can be converted into mathematical models by means of D-H Transformations. The position of the neighbouring joint is the homogeneous matrix between the two coordinates which is given by$T_{i-n} =$

$$\begin{pmatrix} cos\theta & -sin\theta \cdot cos\alpha & sin\theta \cdot sin\alpha & a \cdot cos\theta \\ sin\theta & cos\theta \cdot cos\alpha & -cos\theta \cdot sin\alpha & a \cdot sin\theta \\ 0 & sin\alpha & cos\alpha & d \\ 0 & 0 & 0 & 1 \end{pmatrix}$$

The overall kinematic equation of the single limb is given by:

$$T_{0-5} = T_{0-1} * T_{1-2} * T_{2-3} * T_{3-4} * T_{4-5} = [\ T_{i-n}\ ]$$

While Kinematics involves the design and analysis of the position of a manipulator in 3D coordinate given with the joint actuations, the inverse kinematics computes the 'θ' value for a given 3D Coordinate(x, y, z). As posture and gait coordination could be achieved by controlling the joint angle – which in turn controls the maneuverability. On solving the various equations we obtain the values of – Joint angle to be actuated 'θ' The posture stability is nothing but the robot being adjusting itself in such a way that the Centre

of gravity remains intact while walking on any kind of surface. The pressure center of ZMP and the counter-force of feet from the ground will be coincident when the biped robot is in the movement balance. On excluding the inertial forces for slow speed conditions, the stabilization along the X, Y coordinates are

$$Y_{Stablized} = \frac{\sum_{i=1}^{n} m_i\, gy_i}{\sum_{i=1}^{n} m_i\, g} X_{Stablized} = \frac{\sum_{i=1}^{n} m_i\, gx_i}{\sum_{i=1}^{n} m_i\, g}$$

Fig 2 –graph showing the comparison between standard control and control achieved

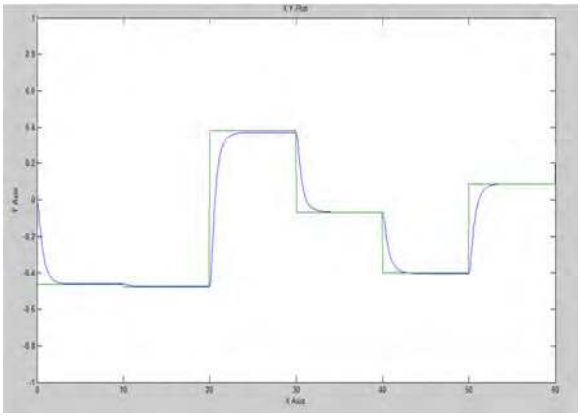

The overall system involving the proposed algorithm are tested using a bipedal prototype, the prototype is designed in such a way that it mimics the exact model of the exoskeletal. The expected result out of the system is compared with the obtained one over time. The graph shows that the formulated control model has an outcome very close to the expected outcome it requires further optimization for dynamic stability

4.Interpretation

It incurs from the output that the robustness of the system has to be improved. The steep advancement in the achieved control has to be progressive, in order to optimize the system further - the real time model has to have more sensory feedback than the illustrated model. The tracking and robustness can be improved in later stages by measuring the event status discretely. The project has advanced to better stages than the exemplified model, the model derived as of now is far reliable than its counterpart included with advanced mechanics and the dynamic control algorithm is being upgraded by improving both static and dynamic stability while generating gait trajectory. By the completion of this project a full-fledged exoskeleton capable of generating its own gait with adaptive control can be realized. It will also serve as a feasible intelligent system that requires less manual control aiding people suffering from paraplegia.

5. References

(2011). *Spinal Cord Injury Facts and Figures at a Glance*. Available: https://www.nscisc.uab.edu

R. Bogue, "Exoskeletons and robotic prosthetics: a review of recent developments," *Industrial Robot: An International Journal,* vol. 36, pp. 421-427, 2009.

P. B. Butler, R. E. Major, and J. H. Patrick, "The technique of reciprocal walking using the hip guidance orthosis (hgo) with crutches," *Prosthetics and Orthotics International,* vol. 8, pp. 33-38, 1984.

G. K. Rose, "The principles and practice of hip guidance articulations," *Prosthetics and Orthotics International,* vol. 3, pp. 37-43, 1979.

G. Baardman, M. J. Ijzerman, H. J. Hermen, P. H. Veltink, H. B. K. Boom, and G. Zilvold, "The influence of the reciprocal hip joint link in the Advanced Reciprocating Gait Orthosis on standing performance in paraplegia," *Prosthetics and Orthotics International,* vol. 21, pp. 210-221, 1997.

Adam Zoss , H. Kazerooni," Design of an electrically actuated lower extremity Exoskeleton," VSP and Robotics Society of Japan 2006, Advanced Robotics, Vol. 20, No. 9, pp. 967

Assistive Robotics for Hemiplegics: Smart Wheel Chairs in Rehabilitative Robotics

Preethika Britto[a] & Sudesh Sivarasu Ph.D [b,]

[a]*Assistant Professor, School of Bio Sciences & Technology, VIT University, India - 632014*
[b]*MRC/MIRU – Division of Biomedical Engineering, Department of Human Biology, Faculty of Health Sciences, University of Cape Town, South Africa 7700* Sudesh.Sivarasu@uct.ac.za

Abstract. Physically disabled persons find their movements very tough with the existing assistive devices. Though there are many robotics available in recent times to enable their motility they require fine and accurate control which is most of the times not possible in cases of higher disability. These robots are very efficient and enable the user to move around with ease. This paper reports the preliminary work in developing a robotic wheelchair system that involves the movement of the shoulder in directing the wheel chair. The system enables the patient to have command over the robot, its direction of movement and will also sense and alarm the user about the obstacles in the path to avoid collision. This wheelchair helps the patient to move in environments with ramps and doorways of little space. This work is based on previous research in robot path planning and mobile robotics, generally a robot should be interactive, and robotic wheelchairs must be highly interactive to enable the system to work most efficiently.

Keywords: Wheel chair automation, Rehabilitation, Shoulder control, Capacitive sensing, Hemiplegic rehabilitation & Ultrasonic intruder sensing

1. Introduction:

Assistive robotics is improving the lifestyle of the physically challenged people to a great extent. In recent times there have been a wide range of assistive and guidance systems available in robotics to make their life less complicated and motile. These robots in are very efficient and enable the user to move around with ease. In recent times there have been various control systems developing specialized for people with various disorders and disabilities. The systems that are developed are highly competitive in replacing the old traditional systems.

There are many assistive systems using visual aids like videooculography systems, infrared oculography, eyeball sensing using electrooculography and much more. There are even systems based on voice recognition too. The basic assisting using voice control is to detect basic commands using joystick or tactile screen. These applications are quite popular among people with limited upper body motility. There are certain drawbacks in these systems. They cannot be used by people of higher disability because they require fine and accurate control which is most of the time not possible. This paper reports the preliminary work in developing a robotic wheelchair system that involves the movement of shoulder kinematics in directing the wheel chair.

The system enables the patient to have command over the robot its direction of movement and will also sense and alarm the user about the obstacles in the path to avoid collision. This wheelchair helps the user to move in environments with ramps and doorways of little space. This work is based on previous research in robotics, generally a robot should be interactive, and robotic wheelchairs must be highly interactive to enable the system to work most efficiently. The whole paper is divided into the following sections. Section 2 describes the principle behind the shoulder movements, Section 3 about the shoulder sensor used, in Section 4 the control system is commented, section 5 shows the ultrasonic intruder sensing mechanism. In Section 6 the overall control system is commented with results.

The choice of sensor: This plays a major role in the sensing mechanism. With reference to various literatures three sensors were narrowed down, Namely Piezoelectric sensor, Strain gauge and the Capacitance sensor. Based on the character stability various tests were performed. The output acquisition rate of the Peizo electric sensor was found to be from 15-23% which was very minute to pick up shoulder

movements. The results of the strain gauge showed that its acquisition rate was 36-59% which was a bit better than the former. The results of the capacitance sensor showed that it could acquire signals at the rate of 80- 90%. Hence Capacitance sensor picked up signals at a better rate. The results are as follows.

Test 1: Output Acquisition:

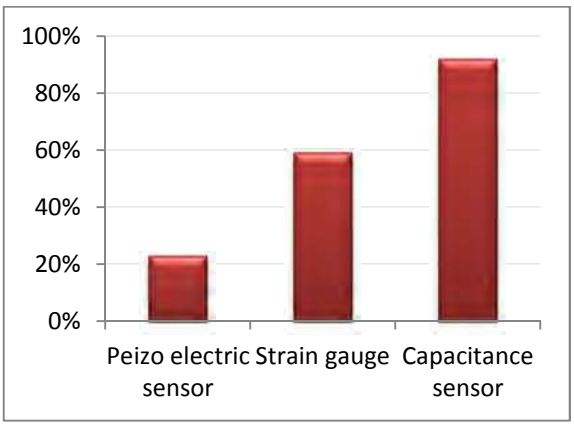

Fig. 1: The output acquisition comparison

Test 2: Accuracy: The accuracy of the output obtained from the three sensors were compared out of which the piezoelectric sensor showed very low accuracy i.e., 20%. The strain gauge showed better results as 80% which was far better, the capacitance sensor showed excellent results as 98%.

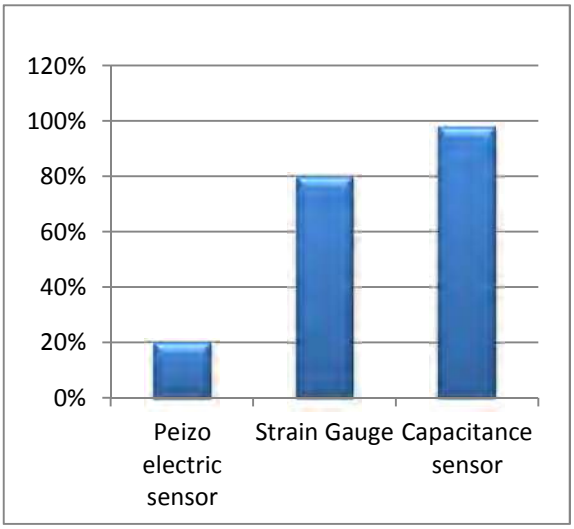

Fig.2: The output accuracy comparison

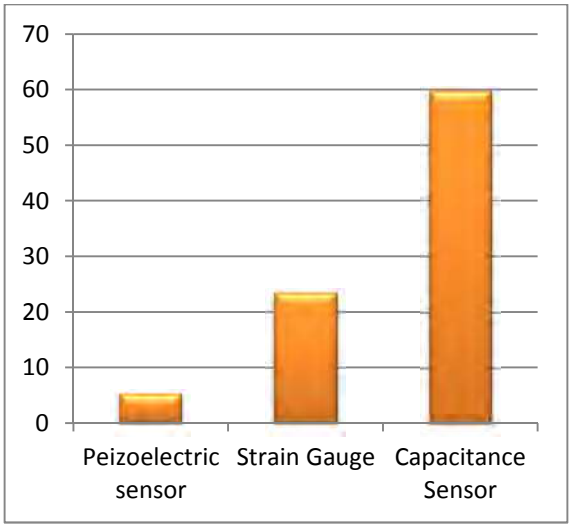

Fig.3: The signal response comparison

The accuracy of the output obtained from the three sensors were compared out of which the piezoelectric sensor showed very low accuracy i.e., 20%. The strain gauge showed better results as 80% which was far better, the capacitance sensor showed excellent results as 98%.

Test 3: Signal Response (in mv)

The sensors were tested for the output signal response. The piezoelectric sensor picked up the signal at 5.3 mv. That implies that this sensor can pick up very low frequencies i.e., even the very low frequency noises can be taken up by the sensor which cannot be suitable for the shoulder. The strain gauge picked up the signal at 23.5 mv which is very minute for shoulder sensing. The capacitance sensor picked up the signal at the 59.5 mv which is optimal for shoulder sensing. So finally after all the tests it was concluded that the capacitance sensor was the suitable one for shoulder sensor.

Principle of shoulder sensing: This sensor is formed by two metallic electrodes wound on a non-metal tube with insulation between electrodes to form much like an open capacitor these electrodes are placed in a feedback loop of a high frequency oscillator. When no material is present inside the tube, the sensor capacitance is low. Therefore, the oscillator amplitude is small. When any material is present, the capacitance value will increase resulting in increased amplitude of the oscillator. Depending on the dielectric constant of the material, the amplitude varies. The evaluating circuit will give the analog output proportional to the dielectric constant of the material.

Table 1: The overall comparison of sensors

Quality	Piezoelectric sensor	Strain gauge	Capacitance sensor
Output acquisition	Very minute (15-23%)	Better (36-59%)	Good (80-92%)
Accuracy	Very low (20%)	Good (80%)	Excellent (98%)
Signal response	Very minute (5.3mv)	Medium (23.5mv)	Good (59.5mv)

When the target approaches the sensor's field, it acts as an electrode to the face of the sensor, and decreases the distance between the electrodes (d), thereby it increases the average surface area of the electrodes. The capacitance with a metal target is always greater than the capacitance of the circuit in the absence of the target. When a non conductive target enters the sensor's field, it acts as an electrical insulator between electrode A and B. The dielectric constant of the material (E) is a measure of its insulation properties. All liquids and solids have a greater dielectric constant than air (E air =1). Therefore the capacitance with a nonmetallic target present is always greater than the capacitance of the circuit in the absence of the target.

Overall Working Mechanism Of Wheel Chair: The wheel chair works in the mechanism of two input one output. Inputs from the eyeball sensor and the pressure sensor placed on the shoulder are taken and antagonistically and fed to the PIC microcontroller which is programmed to move across the direction required.This intellichair is designed to help the paralyzed person who moves on a wheel chair, instead of the handicapped person moving the wheel chair by his hand, the chair will automatically move to a particular direction as the patient moves his eyes towards a direction, with the help of Eye ball movement detection sensor and lifts his shoulder by the shoulder sensor. The chair will also sense the obstacles in front of it and gives a beep sound and stop before it automatically. This is sensed by the ultrasonic sensor. The details regarding the construction of this chair includes the following

Fig:4- Capacitance sensor (shoulder)

Model: A prototype model which symbolizes the wheel chair is constructed using the MS Sheet

Master Controller: A Micro controller will act as a master controller for the movement of the robot. It is responsible for all the decisions taken by the robot.

Eye ball Movement Sensor: This is used to sense the movement of the eye ball's direction and converts it into digital data and transfers it to the Master controller. (Straight Command, Left/Right Command, Stop Command)

Shoulder Movement Sensor: This is used to sense the movement of the shoulder. This is tuned to receive two commands i.e., up and down. This signal is transferred to the Master controller.

Optocoupler with Stepper Driver Board: The need of Opt coupler is to isolate the Interface Board form the Stepper Motor to restrict any high voltage to the Interface board. And this board also contains stepper Driver circuit to amplify the Voltage and to withstand high current because the pulse coming out from the Interface is not tough enough to drive the Motor.

Stepper Power Supply:This board contains the power Supply for the stepper motor and relay driver.

Software Driver in Hitech C: This is a software tool used to control the angular position i.e., to send specified pulses with controlled timing to vary the speed as when and where require

Ultrasonic sensor: Ultrasonic sensor is another way to make non-contact distance measurements. It works by the principle of measuring the time a sound wave takes to propagate from the sensor, to an object and back to the sensor. They are generated by a transmitter and reflected by the target. The returning waves are detected by a receiver. The time delay is used to measure the distance to the object. The farther away an object is, the longer it takes the sound wave to propagate.

This sensor senses the obstacle in the way and stops 30 cm before it. So the wheel chair is fool proof against obstacles on the way of the wheel chair. This

enables the disabled person to move freely around in the environment without any dangers. The patient can be left on their own to move freely in the limited area.

Results: The shoulder sensor was tested with various samples against normal and hemiplegic patients. The following results were obtained, they were found to be almost stable and reliable.

Case 1(a):Normal subjects of different age groups were tested using the shoulder sensor

Case 1(b): The shoulder sensor was tested on a hemiplegic patients and the results were plotted

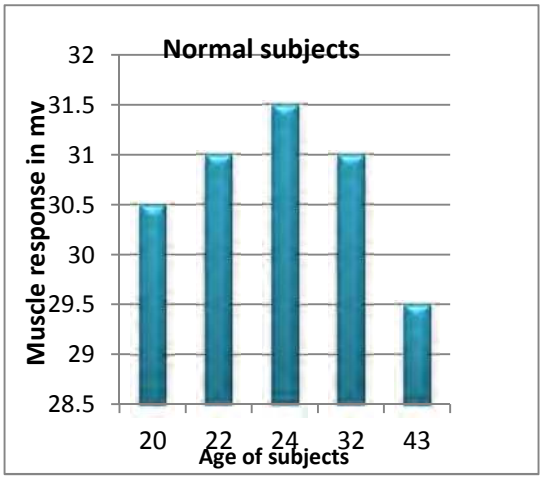

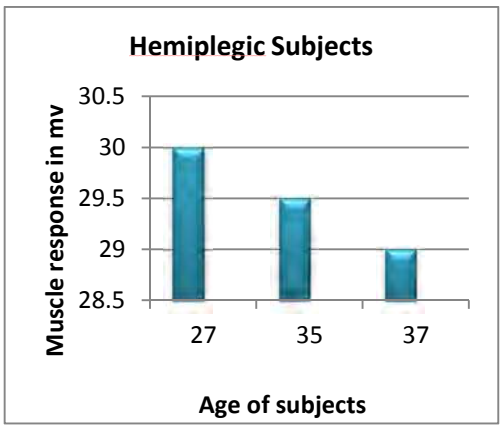

Fig.5 Muscle response of normal(left 1(a)) against Hemiplegic Subjects(1(b))

6.Discussion: Based on the results obtained we conclude that the shoulder response towards normal subjects and hemiplegic patients is very prominent and gives a wide range of movements. Thus the wheel chair moves in all required directions with good response. there is no big difference in the shoulder sensor response when tested on normal subjects and patients i.e., the activity of the sensor depends on the muscle movement of the subject so the range can be narrowed according to the subject using the wheel chair.

7. Conclusion: This work forwards towards the development of a usable, low-cost assistive robotic wheelchair system for disabled people. This system can be used to control the handicapped, especially those with only eye-motor and shoulder coordination, to live more independent lives. Eye and shoulder movements and require minimal effort and allow direct selection techniques, this increase the response time and the rate of information flow. Some of the previous wheelchair robotics research are restricted a particular location and in many areas of robotics, environmental assumptions can be made that simplify the navigation problem. However, a person using a wheelchair and eyeball technique should not be limited by the device intended to assist them if the environment have accessible features.

References

[1] B. Newman and E.T. Liu, Perspective on BRCA1, Breast Disease 10 (1998), 3–10.

[2] D.F. Pilkey, Happy conservation laws, in: Neural Stresses, J. Frost, ed., Controlled Press, Georgia, 1995, pp. 332–391.

[3] E. Wilson, Active vibration analysis of thin-walled beams, Ph.D. Dissertation, University of Virginia, 1991.

End-Effector-Based Robot Assisted Rehabilitation for Upper Extremities

Hennes M. 1), Bollue K. 2), Arenbeck H. 2), Abel D. 2), Disselhorst-Klug C. 1)

1) Department of Rehabilitation & Prevention Engineering, Institute of Applied Medical Engineering, RWTH Aachen University, Aachen
2) Institute of Automatic Control, RWTH Aachen University, Aachen

Introduction

Disability affects near 15% of the people in Europe; around 13.4% of the handicap people in Germany have upper and lower limb impairment. The origin of this injury could be either genetic, by stroke, lesion due sport, or accident. The necessity of therapists, efficient methods, and technology which are able to assist physically disabled individuals has been increasing. In the case of upper extremities, one proposed technology that can satisfy this demand is a robot, which guides the patient´s arm movements. In exoskeletons, every segment of the patient´s arm is attached and controlled by the robot. This is in contrast to the end-effector-based approaches, in which just one distal point of the patient´s arm is attached to the robot. Through this the patient is enabled to perform movements of each arm section autonomously. This paper will approach the use of the robot as an end-effector-based therapy assistance system for upper extremities rehabilitation.

Methods

The patient´s wrist is attached to the robot´s end actuator, which will hold and guide the hand to specific trajectories and positions. The principle of the robot assistance follows mainly three steps: Teaching, where the physiotherapist guides the patient´s upper limb together with the robotic arm, while the movements and positions are being recorded by the robot´s system; Exercise, where the robot, together with the patient´s arm, will repetitively perform the movements and positions as they were recorded during the Teaching phase; Supervision, where inertial sensors detect the patient´s performance during the rehabilitation procedure, in order to detect incorrect movements and ensure the patient´s safety and well execution of the therapy.

Conclusion

The repeatability of the robot offers a constant and precise performance during the therapy, which achieves the movements as they are needed with no alterations. The data obtained from the robot and the sensors done during the supervision, will allow to make a punctual evaluation of the exercise.

Automatic detection of detrusor contraction – Signal analysis of manometric data from pelvic neuromonitoring in minimal invasive surgery

C. Wegner[1], K. H. Somerlik-Fuchs[1], T. B. Krueger[1], R. Mattmueller[1], B. Vondenbusch[2], W. Kneist[3]
[1]inomed Medizintechnik GmbH, Emmendingen, Germany
[2]Hochschule Furtwangen, Furtwangen, Germany
[3]Klinik für Allgemein-, Viszeral- und Transplantationschirurgie, Universitätsmedizin der Johannes Gutenberg Universität Mainz
C.Wegner@inomed.com

Introduction

During surgeries like the resection of a tumor in the rectum, pelvic neuromonitoring allows protecting the autonomous nerves of the minor pelvis. This method can help to improve the functional outcome for patients. By manometry of the urinary bladder the function of the M. detrusor vesicae is monitored. During laparoscopic surgeries artifacts occur in the manometry, which can be ascribed to the respiratory movement of the diaphragm. These artifacts make it more difficult to interpret the manometric signals. Goal of this work was the development of signal processing methods to analyze and measure the artefacts due to laparoscopic intervention. Later this investigation aims towards an automatic detection of the detrusor contraction.

Methods

To remove artifacts a reference signal was generated and combined with the signal of bladder manometry. One approach was the recording of respiratory movement by means of a breathing belt. With a second approach a differential pressure measurement was realized by acquiring bladder pressure in relation to the pressure in the abdomen. Another solution was the implementation of pattern recognition algorithms. This method allows displaying the probability for a reaction of the detrusor in percent. This corresponds to an automatic detection of successful stimulation of the detrusor innervating nerves.

Results

Promising results were obtained for all approaches. An automatic detection of detrusor contraction by pattern recognition however meets the demand of usabiltiy and prevention of misinterpretation of signals particularly well. Automatic detection rates of a detrusor innervation of up to 98 % could be realized with this method.

Conclusion

Hence a user-friendly automatic detection of detrusor contraction even in laparoscopic surgeries can be realized best by pattern recognition.

Optimization of prosthetic alignments with a mobile gait analysis system

Thiele J[1], Westebbe B[1], Kraft M[1]

[1]Technische Universität Berlin, Germany

julius.thiele@tu-berlin.de

Introduction: The prosthesis alignment is of central importance for a harmonic gait, especially for upper limb amputees. Today alignment optimization is based on static measuring and the experience of the orthopaedic technician.

Methods: To objectify the alignment process a mobile gait analysis system based on 10 inertial sensors and a 6 DOF force and moment sensor was developed at the TU Berlin. The dedicated software adds dynamic gait parameters into the optimization process and guides the necessary changes in the prosthesis alignment. Therefore common alignment changes were analysed based on measurements with 7 transfemoral amputee subjects fitted with the C-Leg prosthetic knee joint. For validation purposes all measurements were conducted in a gait lab. The collected data of the different sources is synchronized and physical properties like joint angles, joint moments, energy expenditure and the load line are calculated. Inertial sensors on both feet are used to detect the gait phases. Based on the forces and moments measured in the prosthesis a step detection and filter has been implemented.

Results: Measured kinetic and kinematic data showed a high validity compared to a conventional gait analysis system (Vicon® MX Motion Capturing, AMTI® force plates). Strong inter- and intra-subject variability could be determined. Hence a first measurement with an alignment based on manufacturers' instructions is necessary, acting as a reference for the alignment guiding process. Gait parameters that are consistent over all subjects could be identified for the knee axis position in the sagittal plane. The adaptation of the anterior-posterior knee position is one of the most common alignment modifications and correlates with the maximum of the sagittal moment measured at the knee during terminal stance phase. By means of these findings a first alignment recommendation for the knee in the sagittal plane could be given by the software.

Keywords: amputee; upper limp; prostheses alignment; alignment optimization; mobile gait analysis;

Velocity Vector Field Control of the Omnidirectional Rehabilitation Robot Reha-Maus

S. Knuth[1] and T. Schauer[1]
[1]Technische Universität Berlin, Control Systems Group, Berlin, Germany, sven.c.knuth@campus.tu-berlin.de

Introduction

The table-placed robot Reha-Maus is used for the rehabilitation of arm and shoulder after stroke. The device is indented to guide the patient's lower arm along predefined paths and to support the movement if necessary. Due to the high cost of force sensors, a control concept entirely relying on position and velocity information is investigated.

Methods

The desired path together with its preferred direction to follow and the best way from an arbitrary position onto the path are encoded in a velocity vector field. The robot is equipped with a velocity controller that obtains its reference from the vector field depending on the current position. In order to compensate system friction, the length of all vectors will be increased in a calibration phase until a movement occurs. Ninety per cent of this value is used as base length. To emulate a larger system's inertia, the length of field vectors can be defined as a function of the measured velocity vector. When the patient initiates no movement, support can be given by temporarily increasing the lengths of the field vectors.

Results

To validate the control concept, a desired circular path has been encoded in a velocity vector field, allowing a movement in clockwise direction. Additionally, the vector field realized a rectangular workspace restriction. The system was successfully tested by two healthy subjects who provided only driving forces to the robot for one half of the circle while using the energy stored by the robot's virtual inertia and the guidance provided by the vector field to complete the remaining half of the circle without muscle activity.

Conclusion

A force-sensor-less control concept for the Reha-Maus has been realised successfully. The system guides and supports movements of a patient along predefined paths. Future work involves the validation with stroke patients.

Use of an Inter-Phase Pause to Increase the Efficiency of Biphasic Pulses on Transcutaneous Electrical Stimulation

J.L. Vargas Luna[1,2], M. Krenn[1], J.A. Cortés Ramírez[2], W. Mayr[1]
[1]Center for Medical Physics and Biomedical Engineering, Medical University of Vienna, Vienna, Austria, e-Mail: joseluis.vargasluna@gmail.com
[2]Centro de Innovación en Diseño y Tecnología, Tecnológico de Monterrey, Monterrey, Mexico

Abstract

Nowadays, most of the available devices for transcutaneous electrical stimulation (TES) apply biphasic (BP) pulses. It had been reported that the application of an anodic phase immediately after the cathodic (stimulating) phase may reduce or suppress the neuromuscular fibers response. The use of an inter-phase pause, or break (BR), on conventional BP pulses is studied as a feasible solution to this problem. It is found that such pause effectively induce a difference in the muscle response. The effect slightly increases the immediate muscle response (M-wave and twitch) and strongly increases the H-reflex response recordings. This could be used to decrease the actual electrical doses required, reducing TES-therapies side effects like pain, alterations in the sub-muscle structures and risk of tissue damage due high current-densities. Moreover, it could also lead to increased selectivity and efficiency in activating afferent fibers in the mixed peripheral nerve and thus to methodological improvements.

1 Introduction

Electrical Stimulation (ES), in all its variations, is a powerful and widely used tool for therapy, research and diagnostic. Several techniques have been developed in order to improve quality life of many patients, but some of them are limited to a cohort of patients or time of application due lack of neural selectivity, low performance, alterations in the sub-muscle structures (*e.g.* abdominal muscles stimulation), as well as the induced pain and fatigue of conventional electrical pulses.

Nowadays, most of the available devices for transcutaneous electrical stimulation (TES) apply biphasic (BP) pulses. The main reason for it is that, unlike monopolar stimulation, it delivers a zero net-charge, what provides biocompatibility by avoiding electrode corrosion and tissue damage [1]. Preliminary data show that biphasic (cathodic first) pulses produce a smaller muscle response than monophasic cathodic pulses. Similar observations had been reported on *in vitro* studies and in cochlear stimulation [2], [3]. They reported that with the inclusion of a compensation phase, there is a "vulnerable" period where the action potential may be reduced or avoided. The mathematical model introduced by Rattay [4]–[6] provides a feasible explanation to the phenomenon. Due the fact that action potentials (AP) are triggered along the whole pulse, if an AP is fired just before the phase change, the subsequent anodic phase will promote a hyperpolarizing zone, described by the activation function [5], that could suppress the AP's propagation. A proposed solution is implement an inter-phase pause, or break (BR), to allow the AP to propagate out of the central hyperpolarization region of the anodic phase, what is supported by the findings of [2] (Fig. 1).

Because most of the available stimulators use biphasic stimuli and the addition of a pause between the phases is (relatively) technically easy, a validation of potential improvements of stimulus efficiency by introduction of inter-phase pauses is intended to provide better intensity-outcome relation for actual and future devices and therapies.

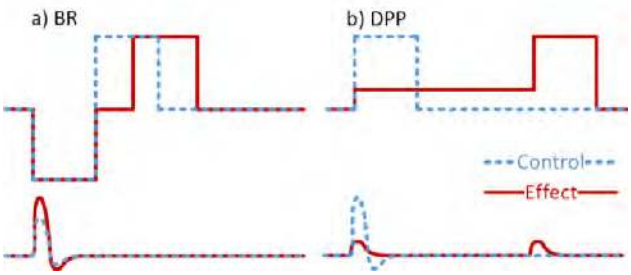

Figure 1 Idealized response differences for non-conventional waveforms under in vitro anodic stimulation. a) Inter-Phase pause or break (BR) and, b) depolarizing pre-pulse (DPP, adapted from [7]).

2 Methodology

Transcutaneous Neuromuscular Electrical Stimulation (NMES) was applied unilaterally to the right tibial nerve (at the level of the *fossa popliteal*) in four neuromuscular-intact volunteers. The test was repeated in one volunteer to test intra-repeatability. The subjects were asked to lie down in prone position, and multimedia material was provided to keep them relaxed during the whole session. The measurements were performed in a quiet, low-light and temperature-controlled room [8]. In the measurements, TES pulses were applied at two different amplitudes (between 10 and 35mA, depending on the subject) where neither of the output signals was saturated. Ten inter-phase pause durations (PWBR) were tested (0, 50, 75, 100, 250, 500, 1000, 2500 and 5000µs, + monophasic pulse, ∞µs), and ten repetitions per combination were given with a 5s

pause between them. The order of the 200 pulses was randomized. The inter-phase pause durations (PWBR) were selected based on the required time for an AP to propagate along the hyperpolarization zone generated by the anodic phase. Based on the geometry of the polarization zones described by the activation function for an idealized case of monopolar stimulation [5], with a nerve distance to active point electrode of ~25mm and a conduction speed of ~45.6m/s [9], the AP requires ~383µs to move away the hyperpolarization zone. However, as Honert & Mortimer reported on the effect of shorter pauses on *in vitro* studies [2], BR durations from 50µs were also included. On the other side we limited the maximum to 5ms since longer pauses could overlap the second phase with the M-Wave.

The stimulation output was monitored via the evoked M-Wave, H-Reflex and muscle twitch movement (MO) recordings from soleus muscle (SO). A pair of electrodes was placed centrally over the soleus muscle belly after skin preparation, while the reference electrode was placed above the anterior tibia. A piezo-electric pulse transducer (1010, UFI, USA) was placed above the longitudinal center of the SO muscle (between the gastrocnemios) to detect the twitch contraction. Both signals were acquired with a MP35 acquisition system (Biopac Systems Inc., USA) at 2.5kS/s.

Monopolar cathodic electrical stimulation was applied transcutaneously using self-adhesive hydrogel electrodes (Hivox Biotek Inc., Taiwan). The reference electrode (5x10cm) was placed in the anterior thigh, slightly above the *patella*. The ideal position of the active electrode was defined giving stimuli (with single test pulses at ~15mA) around the *fossa popliteal* area with a spherical stainless-steel (diameter 2.5cm) electrode (with conductive gel applied over the skin area), until the evoked M-wave and H-reflex were satisfactory. Then, a self-adhesive electrode (2.5cm diameter) was placed accordingly. The stimulation system consisted of a STMISOLA end stage (Biopac Systems Inc., USA), controlled via NI MyDAQ (National Instruments Corp., USA). The whole system was controlled/monitored via a software interface programmed in LabView™ (National Instruments Corp., USA).

For each stimulation amplitude the data were normalized with the average value detected for the control pulses (biphasic with no pause). A statistical analysis was done to prove the significance of the BR effect. First, a Kolmogorov-Smirnov test was run to prove normality on the repetitions of each combination of subject and pause duration (PWBR). Then, a Bartlett test was run to prove variance homogeneity between PWBR groups. Because different variances were expected due subject's inter-variability, the Kruskal-Wallis test was used as non-parametric equivalent to the analysis of variances. Finally, as the Kruskal-Wallis test showed a significant difference between PWBR groups, and most of the sets were normally distributed, the confidence intervals were estimated in order to appreciate the BR effect. The entire statistic test assumed a significance level of α=0.05.

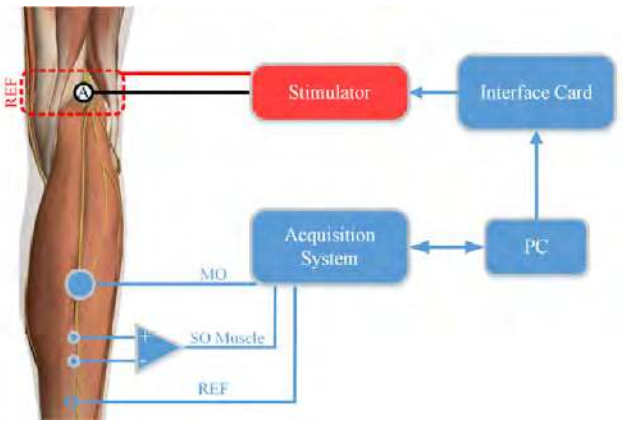

Figure 2 Experimental setup. Cathodic stimuli are applied to the tibial nerve and evoked myoelectric and mechanical responses of the soleus muscle are monitored. Adapted from [10].

3 Results and Discussion

The repetitions result for each group show, in general, a normal distribution but, as expected, the variances are not equal. A total of 1000 samples (divided in 10 PWBR groups) per muscle response signal were computed. The Kruskal-Wallis test shows that significant differences exist between the groups of PWBR variants (Table I). The effect of PWBR variation is shown in Fig. 3.

Table I Statistics results for the BR effect.

Signal	Kruskal-Wallis	Normality	Equal Variances
M-Wave	p-Value≈0	96%	p-Value≈0
H-Reflex	p-Value≈0	84%	p-Value≈0
MO	p-Value≈0	84%	p-Value≈0

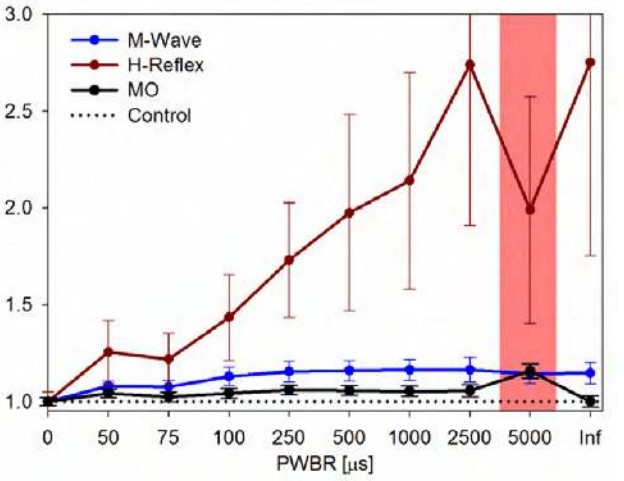

Figure 3 PWBR effect on the normalized Soleus (SO) M-Wave, H-Reflex and muscle twitch (MO). Mean with the 95% confidence interval.

It is shown that the inclusion of an inter-phase pause on biphasic pulses increase mainly the H-reflex, but also slightly the M-Wave and twitch. For the M-Wave, the effect appears to saturate at 100µs, while for H-reflex the results suggest that longer pauses increase the stimulus reaction. It is likely that this effect saturates at PWBRs above out investigation range, since data with "infinite" pause duration (as monophasic pulses may be seen) suggest a saturation known as rheobase (Fig. 3). Additionally, considering nerve conduction speeds and the timing of the muscle response, we had limited the inter-phase pause to less than 5ms, because of expectations that, at large amplitudes, the anodic phase could trigger a second M-Wave. This is supported by recordings in Fig. 4, where M-Wave shape is substantially different for a 5ms-pause. Because of this reproducible observation, the results for such pause duration are invalid (shadow zone in Fig. 3), since obviously a completely different recruitment pattern is achieved.

The results support the theory that the inclusion of an inter-phase pause allows the AP, initiated during the cathodic phase, to propagate out from the hyper-polarize region that the subsequent anodic phase generates. If we assume that the cathodic phase is the stimulating one, it is somehow logical to assume that inverse the phases order (anodic first) may avoid the AP suppression after the cathodic phase. In addition, there is evidence that the charge injection, due a leading anodic impulse, could help to reduce the skin-electrode impedance for a following cathodic stimulating impulse. However, preliminary tests show that use of an anodic-first pulse can also reduce the muscle response. Probably because it can induce a pre-depolarization of fibers (DPP, Fig. 1b), which presumably reduce the excitability due the conditioning of the non-linear conductance of neural sodium channels [11].

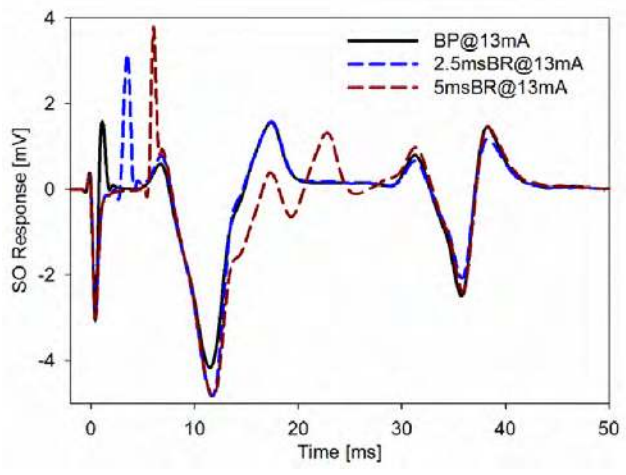

Figure 4 Effect of the inter-phase pause duration with 13mA biphasic stimuli on subject S9.

4 Conclusion

The results shown that an inter-phase pause, inserted in a TES stimulus, is able to induce similar effects on the stimulation outcome than observed earlier in *in vitro* studies [2]. Increasing the pause duration can increase muscle reactions but with the limitation that delays above 5ms (for our specific setup) initiate a second M-Wave in the same stimulus reaction, which may interfere with the study objectives.

Finally, our study demonstrates that the inclusion of an inter-phase pause slightly increases the immediate muscle response (M-wave and twitch) and strongly increases the H-reflex response recordings. Although additional validation must be done for other configurations, this could be used to decrease the actual electrical doses required, reducing TES-therapies side effects like pain, alterations in the sub-muscle structures and risk of tissue damage due high current-densities. Moreover, it could also lead to increased selectivity and efficiency in activating afferent fibers in the mixed peripheral nerve and thus to methodological improvements.

5 References

[1] D. R. Merrill, M. Bikson, and J. G. R. Jefferys, "Electrical stimulation of excitable tissue: design of efficacious and safe protocols.," *J. Neurosci. Methods*, vol. 141, no. 2, pp. 171–98, Feb. 2005.

[2] C. Honert and J. T. Mortimer, "The response of the myelinated nerve fiber to short duration biphasic stimulating currents," *Ann. Biomed. Eng.*, vol. 7, no. 2, pp. 117–125, Mar. 1979.

[3] J. T. Rubinstein, C. A. Miller, H. Mino, and P. J. Abbas, "Analysis of monophasic and biphasic electrical stimulation of nerve," *IEEE Trans Biomed Eng*, vol. 48, no. 10, pp. 1065–1070, 2001.

[4] F. Rattay, "Analysis of models for external stimulation of axons," *Biomed. Eng. IEEE Trans.*, no. 10, pp. 974–977, 1986.

[5] F. Rattay, "Analysis of models for extracellular fiber stimulation.," *IEEE Trans. Biomed. Eng.*, vol. 36, no. 7, pp. 676–82, Jul. 1989.

[6] F. Rattay, "Current distance relations for fiber stimulation with pointsources.," *IEEE Trans. Biomed. Eng.*, vol. 55, no. 3, pp. 1122–7, Mar. 2008.

[7] W. M. Grill and J. T. Mortimer, "Inversion of the current-distance relationship by transient depolarization.," *IEEE Trans. Biomed. Eng.*, vol. 44, no. 1, pp. 1–9, Jan. 1997.

[8] R. M. Palmieri, C. D. Ingersoll, and M. A. Hoffman, "The hoffmann reflex: methodologic considerations and applications for use in sports medicine and athletic training research.," *J. Athl. Train.*, vol. 39, no. 3, pp. 268–77, Jul. 2004.

[9] K. M. Galloway, M. E. Lester, and R. K. Evans, "Clinical utility of tibial motor and sensory nerve conduction studies with motor recording from the flexor hallucis brevis: a methodological and reliability study.," *J. Foot Ankle Res.*, vol. 4, no. 1, p. 14, Jan. 2011.

[10] Zygote Media Group Inc., "Zygote Body & 3D Data," 2012. [Online]. Available: www.ZygoteBody.com.

[11] W. M. Grill and J. T. Mortimer, "Stimulus waveforms for selective neural stimulation," *IEEE Eng. Med. Biol. Mag.*, vol. 14, no. 4, pp. 375–385, 1995.

A Versatile Stimulator for Advanced Transcutaneous FES Applications Enabling User-Specified Pulse Waveforms

M.Valtin[1], K. Kociemba[2], C. Behling[2], B. Kuberski[2], M. Weber[2], T. Schauer[1]
[1]Control Systems Group, Technische Universität Berlin, Berlin, Germany, valtin@control.tu-berlin.de
[2]Hasomed GmbH, Magdeburg, Germany

Abstract

Functional Electrical Stimulation (FES) is a commonly used method in clinical rehabilitation and research to trigger muscle contractions by electrical stimuli, e.g. applied via self-adhesive surface electrodes. A variety of stimulation systems is commercially available which all offer limited control over the stimulation waveform and timing. In this work, a stimulation system is presented, which allows extensive control over the stimulation waveform and the stimulation timing. Additionally, the stimulator supports array electrodes and enables surface electromyography (sEMG) measurements. The waveform is entirely user defined by declaration of characteristic points of the waveform which will be piecewise constant interpolated. Up to 16 points can be declared, each with a duration ranging from 10 µs up to 4095 µs and a current of up to +/- 150 mA. A symmetric, balanced biphasic waveform as well as a balanced triangular waveform were used to validate the waveform generation. To validate the stimulation timing, which is also entirely user defined, a real-time operating system was used. Recording of sEMG signals from the stimulation electrodes is possible even during active stimulation because of the high voltage protection of the EMG analogue frontend. To demonstrate the use in advanced FES applications, a drop foot stimulation experiment was conducted using a novel stimulation waveform. The designed waveform enables almost independent control of the muscle fibularis longus and the muscle tibialis anterior with only a single stimulation channel.

1 Introduction

Functional Electrical Stimulation (FES) is a well-known technique for rehabilitation of stroke survivors or patients with spinal cord injuries. FES is also used for cardiovascular training on paraplegic patients while research continuously extends the spectrum of FES applications.

Today the transcutaneous FES setup usually consists of a stimulation device, at least two self-adhesive surface electrodes and some kind of sensor to control the stimulation. The stimulation device usually generates symmetric, or unsymmetrical, charge balanced, and current controlled stimulation pulses with adjustable pulse width and current. Usually, the adjustable stimulation parameters are very limited in these systems to simplify operation in daily use by non-technically trained staff.

Optimal stimulation results strongly depend on a good electrode placement. Surface electrodes in contrast to implanted electrodes do not require any surgery. Instead these electrodes need to be placed on top of the skin, above the motor point of the desired muscle, or above the nerve, which innervates the desired muscle through the motor point.

The placement of surface electrodes is error-prone because the placement has to be repeated before every FES application and validation is difficult. Another inconvenience in FES application is muscle fatigue which occurs a lot faster than normal, because the stimulation impulses always contracts the same selection of muscle fibres.

Current research addresses both problems with array electrodes, which have more but smaller stimulation elements on a single self-adhesive gel layer [1]. These electrodes require an external demultiplexer to connect individual elements or an element selection with the stimulation device [2]. Another subject of current research is the utilization of electromyography (EMG) signals, which contain information about the muscle activity. EMG is often used to trigger the stimulation which increases the rehabilitation success (see e.g. [3]) or for feedback purposes. EMG can also be used to detect muscle fatigue and to adjust the applied stimulation intensity [4]. EMG signals are usually recorded from two EMG electrodes (different from the stimulation electrodes) and by using an external EMG amplifier, although commercial systems begin to include EMG measurement capabilities into the stimulation device. The EMG electrodes need to be placed near to the stimulation electrodes to measure the electrical signals from the stimulated muscle. This is a problem for array electrodes which are larger than normal electrodes and do not allow such a placement of the EMG electrodes. None of the current commercially available stimulation systems allows EMG measurements over the stimulation electrodes during active stimulation as proposed in [2,5].

This contribution introduces a novel stimulation system with integrated EMG measurement over the stimulation electrodes also during active stimulation, with support for array electrodes and with precise control over every aspect of the stimulation waveform.

As an example for an advanced FES application, which is now possible, a drop foot stimulation is shown using a novel stimulation waveform. FES applications often require more than one muscle to be stimulated. This can be the antagonist of a specific muscle like in FES cycling (see e.g. [1]) or a completely different muscle like in the drop

foot applications [6, 7]. This is normally achieved by two or more stimulation channels, each with two electrodes. Usage of only one electrode close to the motor point of each muscle is not possible because the standard symmetric biphasic waveform stimulates the muscle underneath both electrodes equally. Monophasic waveforms restrict the stimulation effect to one electrode, depending on the sign of the stimulation pulse, which usually cannot be freely chosen. The monophasic waveform is also not recommended for prolonged stimulation because of the remaining charge on the electrodes.

The proposed novel waveform allows for the drop foot stimulation almost independent control of the muscle fibularis longus and the muscle tibialis anterior with only one stimulation channel.

2 Methods

2.1 Stimulation device

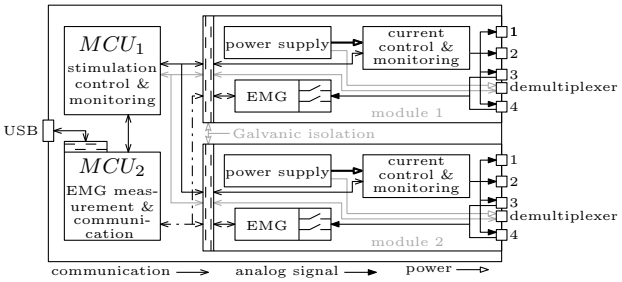

Figure 1 Block diagram of the stimulation system.

An overview of the presented stimulation device is shown in Fig. 1. Two independent, Galvanically isolated stimulation modules feature four current controlled stimulation channels each. Both modules are controlled by the ARM® Cortex©-M4 (STM32F407; STMicroelectronics) microcontroller MCU_1. The microcontrollers sole task is the generation and monitoring of the stimulation waveform, ensuring safe electrical stimulation. For this reason, the microcontroller implements only the well tested low level protocol which describes the stimulation waveform.

Each module uses an analog frontend (ADS1294, Texas Instruments) for sEMG measurements with 4 kHz sampling frequency. The 2x24 bit EMG data is received by the second ARM® Cortex©-M4 (STM32F407; STMicroelectronics) microcontroller MCU_2 which is also connected to an external control unit via a Galvanically isolated USB. The MCU_1 is only connected to the MCU_2 which forwards any received low level commands, or generates new low level commands according to received high level commands.

2.1.1 Adjustable Stimulation Waveform

The key feature of the introduced stimulation system is the extensive level of control over the waveform used for electrical stimulation. The desired waveform can be described by up to 16 characteristic points which will be piecewise constant interpolated. Each point consists of the duration of interpolation t_{di} and the corresponding current level i_i. Future development will also allow other interpolation forms.

In Fig. 2, the configuration for a biphasic pulse, defined by three points, is shown. Any number of waveforms can be created this way. Fig. 3 shows a few examples with the corresponding configuration points. The duration t_{di} of each point can be chosen in between 10 µs and 4095 µs in 1µs steps. The current i_i has a resolution of 0.5 mA and is limited to +/- 150 mA.

The transmission of the largest pulse configuration with 16 points requires about 270 µs. After about 400 µs of additional data processing, the stimulation begins. This timing depends on the number of points, since only the active points are transmitted. The overall duration of one stimulation pulse is composed of transmission plus processing delay and the sum of the configured durations. The exemplary biphasic waveform shown in Fig. 2 with a pulse wide of 300µs therefore has an overall duration of about 1.2 ms. Hence, the resulting theoretical maximal stimulation frequency for this configuration is about 830 Hz, since each stimulation pulse is executed as soon as it is received. This enables a wide range of possible stimulation patterns and a very flexible timing.

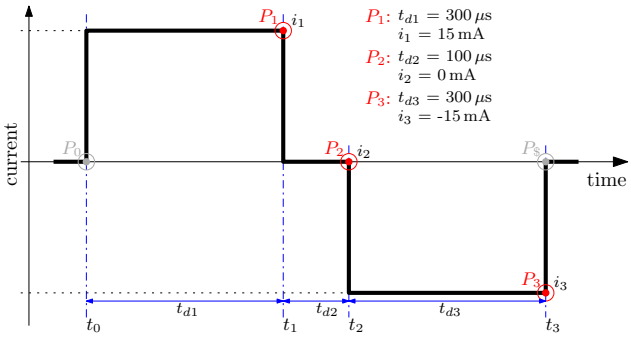

Figure 2 Exemplary biphasic stimulation pulse configuration.

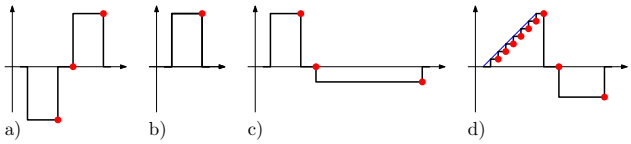

Figure 3 Selection of possible stimulation waveforms.

Multiple pulse configurations can be sent consecutive and will be buffered by the stimulator until they are processed. Buffered pulse configurations will be processed in order of arrival with the exception of pulses, which use different stimulation modules. Two pulse configurations, one for stimulation module 1 and one for stimulation module 2, will be processed in parallel except for the processing delay. An even better synchronisation can be achieved by adding a dummy point with t_{dl} equal to the procession delay and a current of 0 mA as first point to the configuration. This strategy can also be used to ensure a fixed overall pulse duration, which is independent from the desired pulse width.

The drawback of the described flexibility is its complexity that may overwhelm users for daily standard tasks.

To solve this issue a second software layer is introduced which provides simplified commands for common tasks like for example biphasic stimulation with a certain stimulation frequency and pulse parameters. In this scenario the high level commands are received by the microcontroller MCU_2, which translates them into low level commands that are sent to the stimulation microcontroller MCU_1.
This approach allows developing of a well tested, multipurpose stimulation system with an easily adaptable user interface.

2.1.2 Optional Demultiplexer Support

The stimulation system also supports array electrodes through an optional demultiplexer, which was optimized in size (credit card size) to allow an external placement next to the array electrode, eliminating extensive wiring. All necessary support systems like the power supply or the control system are integrated into the stimulator. The demultiplexer configuration is applied once for the entire waveform. The transition duration increases imperceptibly but the processing time increases by about 1ms because the demultiplexer must be set up before any stimulation pulse can be generated.
The number of active array elements or counter array elements can be changed to fit the individual requirements. The demultiplexer offers 30 fixed active array elements, 4 fixed counter array elements and 2 times 13 selectable array elements (either active or counter elements).

2.2 Balanced, Unsymmetrical Drop Foot Stimulation

A round electrode (32 mm diameter) is placed over the peroneal nerve, which mostly innervates the muscle fibularis longus, and an oval electrode (4x6cm) is placed on top of the muscle tibialis anterior. The real-time controller is generated using Scilab and the Hart toolbox (http://hart.sf.net). A PC running Linux with the Rtai real-time extension is used to control the intensities and the waveform of the one stimulation channel used. The GUI QRtaiLab is used for signal monitoring and parameter updates.
One Bluetooth inertial measurement unit (IMU) (RehaWatch, Hasomed GmbH, Germany) is mounted to the foot to determine the dorsiflexion angle α as well as the eversion angle β of the foot. The IMU is attached in an arbitrary orientation. Therefore a calibration movement is used to calculate a correction matrix, which rotates the sensor coordinate system. The corrected accelerometer, gyroscope, and magnetometer data is used to calculate the sensor's orientation using a direction cosine matrix (DCM) algorithm. The resulting Euler angles are used to describe the foot movement caused by the stimulation.

2.2.1 Waveform Definition

Fig. 4 shows the novel waveform that is used. The first part q_1 (positive charge), defined by point 1, is independent from the second part q_3 (negative charge), defined by point 3. A third part q_4, defined by point 4, is introduced to achieve the desired total charge balance. The charge of the third part is therefore defined by

$$q_4 = -(t_{d1} \cdot i_1 + t_{d3} \cdot i_3).$$

The absolute value of the current i_4 is chosen as i_{min} (very small value). This ensures that the pulse defined by q_4 does not generate an additional stimulation response. The current i_4 and the pulse width t_{d4} follow from the charge q_4 by $i_4 = i_{min}\,\mathrm{sign}(q_4)$ and $t_{d4} = \mathrm{abs}(q_4/i_{min})$, respectively. The current i_{min} is set to 4 mA and increased when the pulse width t_{d4} exceeds 4095 µs.

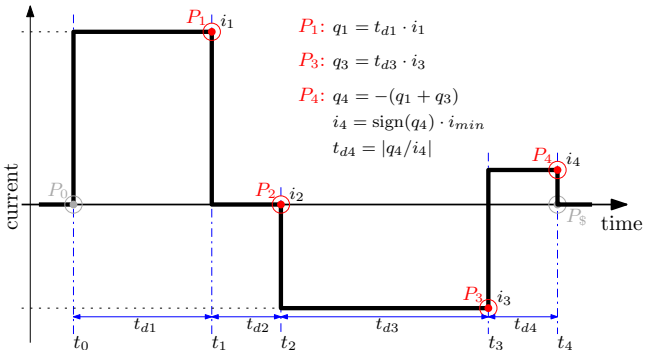

Figure 4 Novel stimulation pulse waveform.

The muscle tibialis anterior, which dominantly evokes dorsiflexion, is mostly activated by the first part of the waveform, referred to as $q_{M1} = q_1 = i_1 t_{d1}$. The muscle fibularis longus evokes dorsiflexion and eversion, and is mostly activated by the second part of the waveform, referred to as $q_{M2} = q_3 = i_3 t_{d3}$. This assigning is valid when the electrode on the muscle tibialis anterior serves first as cathode.

3 Results

3.1 Waveform Generation

A series of tests was conducted to evaluate the waveform generation. The tests used a 1kΩ resistive load to evaluate the timing and the stimulation intensity. Fig. 5 shows the resulting oscilloscope output for two consecutively generated stimulation pulses. The first pulse uses the pulse configuration shown in Fig. 2 with 300µs pulse width and 15mA current. The timing of the individual parts and the timing of the whole stimulation pulse coincide very well with the requested configuration. The same is true for stimulation current of the positive and the negative part, which have both no current overshoot.
The second pulse shown in part in Fig. 5 is the approximated linear ramp from Fig. 3 d). The linear slope is approximated with 14 sampling points, each 21 µs long with a 1 mA current increase.
In between the two pulses is the delay of about 700 µs visible which is related to receiving and processing of second pulse definition.
The consistency of these timings was evaluated be prolonged stimulation with up to 200Hz using a Linux system with the Rtai real-time extension and monitoring of the stimulation pattern.

Figure 5 Generated waveform on a 1kΩ resistive load.

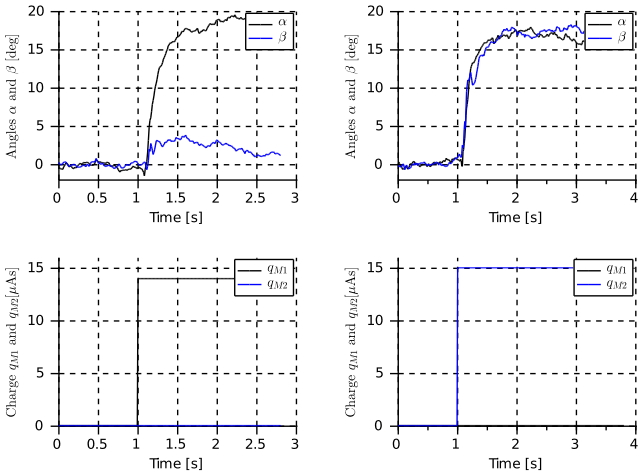

Figure 6 Input step responses of the foot angles.

The demultiplexer functionality was evaluated through a simulated array electrode, which uses LEDs to visualize the current path, and a 500Ω resistive load.

3.1 Balanced, Unsymmetrical Stimulation

In a series of experiments, we evaluated the proposed stimulation waveform on a healthy subject. The person was sitting on a chair with the shank/ foot free to swing.
Fig. 6 shows the step responses for a jump from no stimulation to q_{Mi}, i=1,2, which are the smallest stimulation intensities that produce the largest foot angles without saturation. The left side shows the step response for q_{M1} (muscle tibialis anterior). The third part of the pulse (i_4=-4mA and t_{d4}=3491µs) is well below the stimulation threshold of the muscle fibularis longus.
The right side of Fig. 6 illustrates the step response for q_{M2}. Since the muscle fibularis longus evokes dorsiflexion and eversion, both angles clearly increase. The third part of the pulse (t_{d4}=3748µs and i_4 =4mA) is again unlikely to trigger an additional muscle contraction.

4 Conclusion

A highly configurable stimulation system was presented where specification of up to 16 characteristic points allows generating any number of stimulation waveforms. The timing of the stimulation pattern is also freely definable, as long as the external control is sufficiently fast. To ease the minimum requirements for the external control system, a second, much simpler software layer has been designed.
The stimulator also directly supports array electrodes through an external demultiplexer module and allows EMG measurements over inactive stimulation channels as well as over active stimulation channels. Further work will focus on sEMG filtering during active stimulation.
The usefulness of the unique waveform configuration was demonstrated on a drop foot stimulation use case. A novel stimulation waveform was proposed allowing control over foot dorsiflexion and eversion with only one stimulation channel. In further work, we will use this approach in the feedback control strategies described in [6,7].

5 References

[1] Downey, R., Ambrosini, E., Ferrante, S., Pedrocchi A. and Ferrigno, G.: Asynchronous Stimulation with an Electrode Array Reduces NMES-Induced Muscle Fatigue during FES Cycling, Proc. of the 17th IFESS Conference, 2012

[2] Valtin, M., Schauer, T., Behling, C., Daniel, M. and Weber, M.: Combined stimulation and measurement system for array electrodes, Proc. of Biodevices, pp. 345-349, 2012

[3] Dutta, A., Kobetic, R.and Triolo, R.: Development of an implanted intramuscular EMG-triggered FES system for ambulation after incomplete spinal cord injury, Conf. Proc IEEE EMBS, pp. 6793-6797, 2009

[4] Klauer, C., Raisch, J. and Schauer, T.: Linearisation of electrically stimulated muscles by feedback control of the muscular recruitment measured by evoked EMG, Proc. of the 17th IEEE International Conference on Methods and Models in Automation and Robotics, IEEE, pp. 108-113, 2012

[5] Shalaby, R., Schauer, T., Liedecke, W. and Raisch, J.: Amplifier design for EMG recording from stimulation electrodes during functional electrical stimulation leg cycling ergometry. *Biomedical Engineering*, 56(1), 23–33, 2011

[6] Seel, T., Laidig, D., Valtin, M. and Schauer, T.: Feedback Control of Foot Eversion in the Adaptive Peroneal Stimulator, IEEE Mediterranean Conference on Control and Automation, Palermo, Italy, 2014

[7] Valtin, M., Seel, T., Raisch, J. and Schauer, T., Iterative Learning Control of Drop Foot Stimulation with Array Electrodes for Selective Muscle Activation, Proc. of the IFAC WC, Cape Town, South Africa, 2014

Acknowledgement

This work was conducted within the research project APeroStim, which is supported by the German Federal Ministry of Research and Education (FKZ 01EZ1204B).